ADVANCED ENERGY MATERIALS
www.advenergymat.de

Unity Convoluted Design of Solid Li-Ion Battery and Triboelectric Nanogenerator for Self-Powered Wearable Electronics

*Xi Liu, Kun Zhao, Zhong Lin Wang, and Ya Yang**

Wearable electronics suffer from severe power shortage due to limited working time of Li-ion batteries, and there is a desperate need to build a hybrid device including energy scavenging and storing units. However, previous attempts to integrate the two units are mainly based on simple external connections and assembly, so that maintaining small volume and low manufacturing cost becomes increasingly challenging. Here a convoluted power device is presented by hybridizing internally a solid Li-ion battery (SLB) and a triboelectric nanogenerator (TENG), so that the two units are one inseparable entity. The fabricated device acts as a TENG that can deliver a peak output power of 7.4 mW under a loading resistance of 7 MΩ, while the device also acts as an SLB to store the obtained electric energy. The device can be mounted on a human shoe to sustainably operate a green light-emitting diode, thus demonstrating potential for self-powered wearable electronics.

Wearable electronics have attracted extensive interests due to potential applications in healthcare monitoring and personal sensing.[1,2] Usually, wearable devices include functional sensor part such as GPS sensors and the energy storage unit such as Li-ion batteries. The limited capacity of Li-ion batteries results in difficulty of sustainable operations of these wearable devices. To solve this issue, various nanogenerators by scavenging ambient energies have been exploited to charge Li-ion batteries for increasing sustainable working time of these sensors.[3–7] Among various nanogenerators, triboelectric nanogenerators (TENGs) have been extensively designed to scavenge almost all forms of ambient mechanical energies,[8–11] especially human-motion-induced biomechanical energy owing to the light weight and high output performances.[12–14] Due to the AC output characteristics of TENGs, effective charging of Li-ion batteries can be achieved by utilizing a rectifier between the TENG and Li-ion battery.[15] The simple external connections of the two devices are not beneficial for the decrease of total device size and the lower manufacturing cost. An ideal solution to design a device that is not only a TENG but also an Li-ion battery, thus the two different functional units has common electrodes and can be regarded as one device.

Previous investigations about the combination of TENGs and Li-ion batteries indicate the difficulty of integrating the two different functional units into one device.[16–18] The main reason is that the conventional Li-ion batteries include an anode, a cathode, and a liquid electrolyte to create a completely enclosed environment, where the effective contact–separation of two materials is impossible in the filled liquid electrolyte.[19,20] However, the working of TENGs requires a periodical contact–separation of two different triboelectric materials, so that the TENGs cannot be integrated into conventional Li-ion batteries.[8] To solve this issue, the use of solid Li-ion batteries (SLBs) may provide the possibility of combining the two different functional units into one device. As compared with the conventional liquid electrolyte, the solid electrolyte exhibits a large electrochemical stability and improved safety.[21,22] Moreover, without needing a fully enclosed space, the SLBs can work in atmospheric environment, where the mechanical motions of the Li-ion batteries may be utilized to drive the TENG.

Here, we report a convoluted power (CP) device by hybridizing internally a TENG and an SLB by sharing common electrodes. The SLB consists of TiO_2 nanotubes as anode, the polyethylene oxide–$Li_{(1+x)}Ti_{(2-x)}Al_x(PO_4)_3$ (PEO–LATP) solid electrolyte, and the $LiMn_2O_4$ (LMO) nanoparticles as cathode, where the periodic contact–separation between the TiO_2 nanotubes and the PEO–LATP–LMO membrane is the operation process for the TENG. A circular triboelectric fluorinated ethylene propylene (FEP) film was attached on the PEO–LATP–LMO membrane to achieve a 93-fold enhancement in output voltage of the TENG as compared with no use of the FEP film. The invented CP device as a TENG can deliver an output voltage of about 188 V and an output current of about 33.5 μA with a contact area of smaller than 7.1 cm^2 by scavenging ambient mechanical energy, and the CP device as an SLB can store electric energy with corresponding capacities ranged from 0 to 15 μAh under increased pressures from

X. Liu, K. Zhao, Prof. Z. L. Wang, Prof. Y. Yang
Beijing Institute of Nanoenergy and Nanosystems
Chinese Academy of Sciences
Beijing 100083, China
E-mail: yayang@binn.cas.cn
X. Liu, K. Zhao, Prof. Z. L. Wang, Prof. Y. Yang
CAS Center for Excellence in Nanoscience
National Center for Nanoscience and Technology (NCNST)
Beijing 100190, China
Prof. Z. L. Wang
School of Materials Science and Engineering
Georgia Institute of Technology
Atlanta, GA 30332-0245, USA

DOI: 10.1002/aenm.201701629

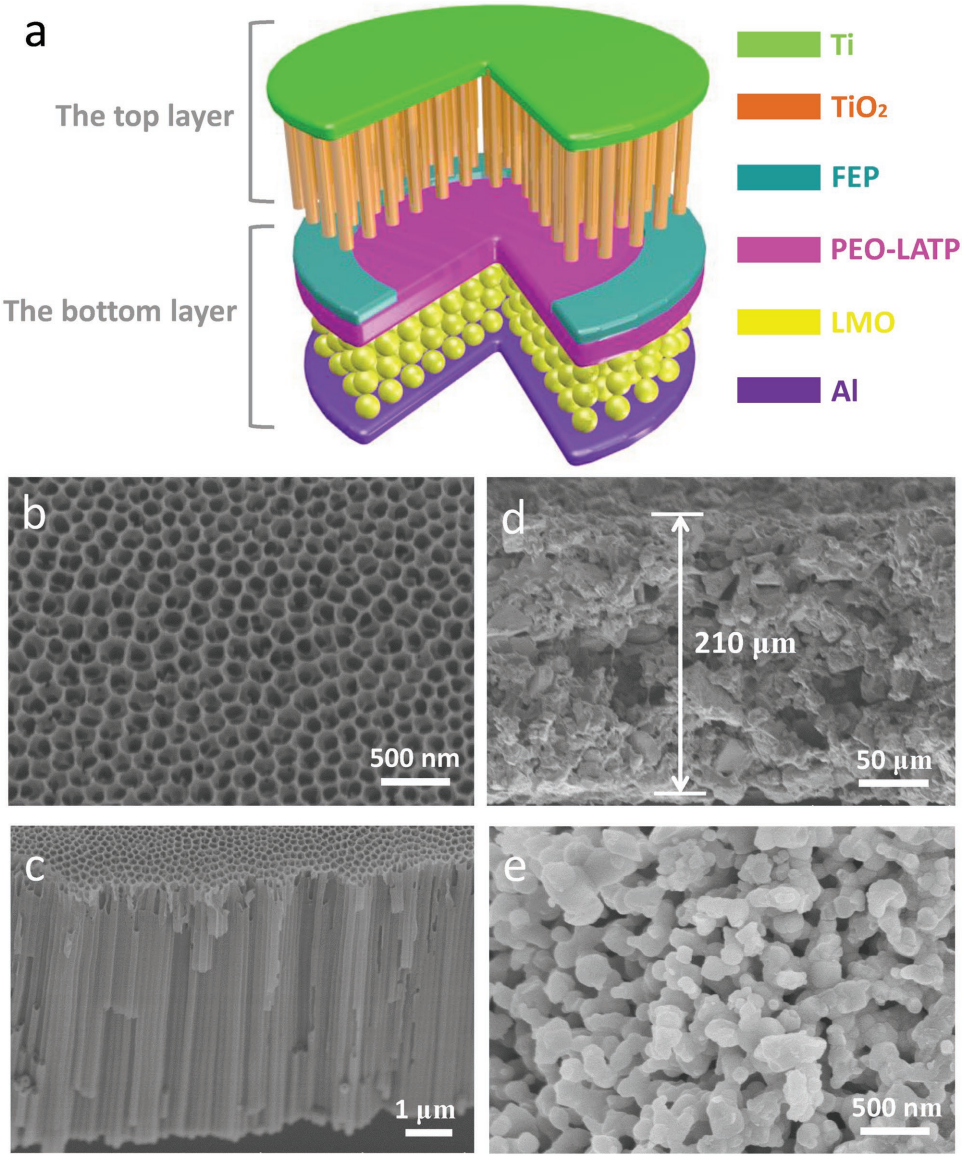

Figure 1. Fabrication of the CP device. a) Schematic diagram of the CP device. b) SEM image of the TiO_2 nanotubes. c) Cross-sectional SEM image of the TiO_2 nanotubes. d) Cross-sectional SEM image of the PEO–LATP electrolyte film. e) SEM image of the LATP nanoparticles.

0 to 30 kg cm^{-2}. Mounted on a human shoe, the fabricated CP device can effectively convert human motions-induced biomechanical energy such as walking into electricity, where the corresponding electric energy can be utilized to directly power some electric devices such a green light-emitting diode (LED) or stored in this device for further sustainably powering wearable electronics.

Figure 1a illustrates the schematic diagram of the CP device with two separated layers. The top layer consists of TiO_2 nanotubes on a Ti foil, which was attached on an acrylic sheet. The bottom layer includes a circular FEP film, a PEO–LATP film, an LMO film, and an Al electrode. Under a pressure applied on the CP device, the TiO_2 nanotubes of the top layer can have a close contact with both the LATP film and the FEP film. As displayed in Figure S1a in the Supporting Information, the CP device has dimensions of 60 mm × 60 mm × 30 mm, where the annular FEP film has the inner and outer diameters of 15 and 30 mm, respectively. Figure 1b presents a scanning electron microscope (SEM) image of the TiO_2 nanotubes and the detailed fabrication information is described in the Methods. The TiO_2 nanotubes have the uniform holes with the diameters of about 120 nm and the length of the nanotubes is about 3.3 μm, as exhibited in Figure 1c. Figure 1d depicts a cross-sectional SEM image of the solid PEO–LATP electrolyte film with a thickness of about 210 μm and a diameter of about 30 mm (Figure S1b, Supporting Information), where the LATP nanoparticles with diameters of about 150 nm were utilized to fabricate the electrolyte film under an applied pressure of about 15–20 MPa, as presented in Figure 1e. The obtained LATP nanoparticles were synthesized by sol gel method and the corresponding X-ray diffraction (XRD) pattern indicates that no impurity can be found, as displayed in Figure S2 in the Supporting Information. Moreover,

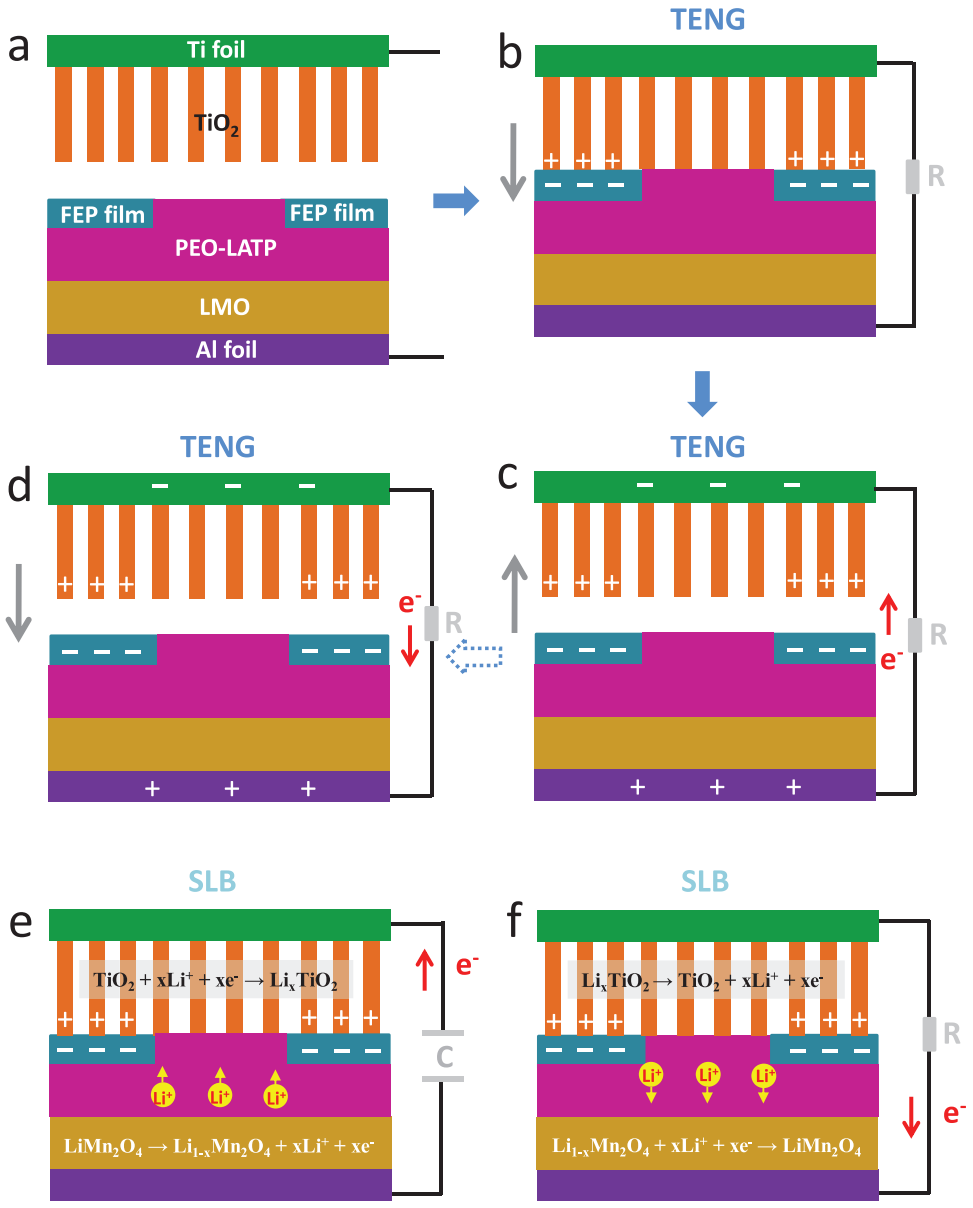

Figure 2. Working mechanism of the CP device as a TENG and an SLB. a) Schematic diagram of the CP device. b) Schematic diagram of the triboelectric charges on the surfaces of TiO_2 nanotubes and FEP film, where the gray arrow represents the movement direction of TiO_2 nanotubes. Schematic illustrations of electric generation for the CP device as a TENG when the TiO_2 nanotubes on Ti foil being moved c) up and d) down. Schematic illustrations of the e) charging and f) discharging processes for the CP device as an SLB, where the SLB can be charged by using a TENG charged capacitor.

the SEM image of the used LMO nanoparticles shows that the diameters of these nanoparticles are smaller than 500 nm, as illustrated in Figure S3 in the Supporting Information.

As displayed in **Figure 2**a–c and Figure S4 (Supporting Information), the power generation mechanism can be understood from the coupling of the triboelectric effect and electrostatic induction. At the beginning, there is no observed output current/voltage when there is a gap between the top layer and the bottom layer, as shown in Figure 2a and Figure S4a (Supporting Information). Under an applied pressure on the CP device, the effective contact between the TiO_2 nanotubes and the FEP film can induce different triboelectric charges on the surfaces of TiO_2 and FEP due to the different triboelectric polarities, as illustrated in Figure 2b and Figure S4b (Supporting Information). Due to the electrostatic induction, the separation between the TiO_2 nanotubes and the FEP film can induce the flow of electrons from bottom Al electrode to top Ti electrode, as presented in Figure 2c and Figure S4c (Supporting Information). After the electric balance has been created, there is no output current or voltage in the external circuit (Figure S4d, Supporting Information). When the pressure was applied on CP device again, the decrease of distance between the TiO_2 nanotubes and the FEP film can induce the flow of electrons from the bottom Al electrode to the top Ti electrode (Figure 2d; Figure S4e, Supporting Information), thus the TENG exhibits AC output signals. The effective contact between the TiO_2

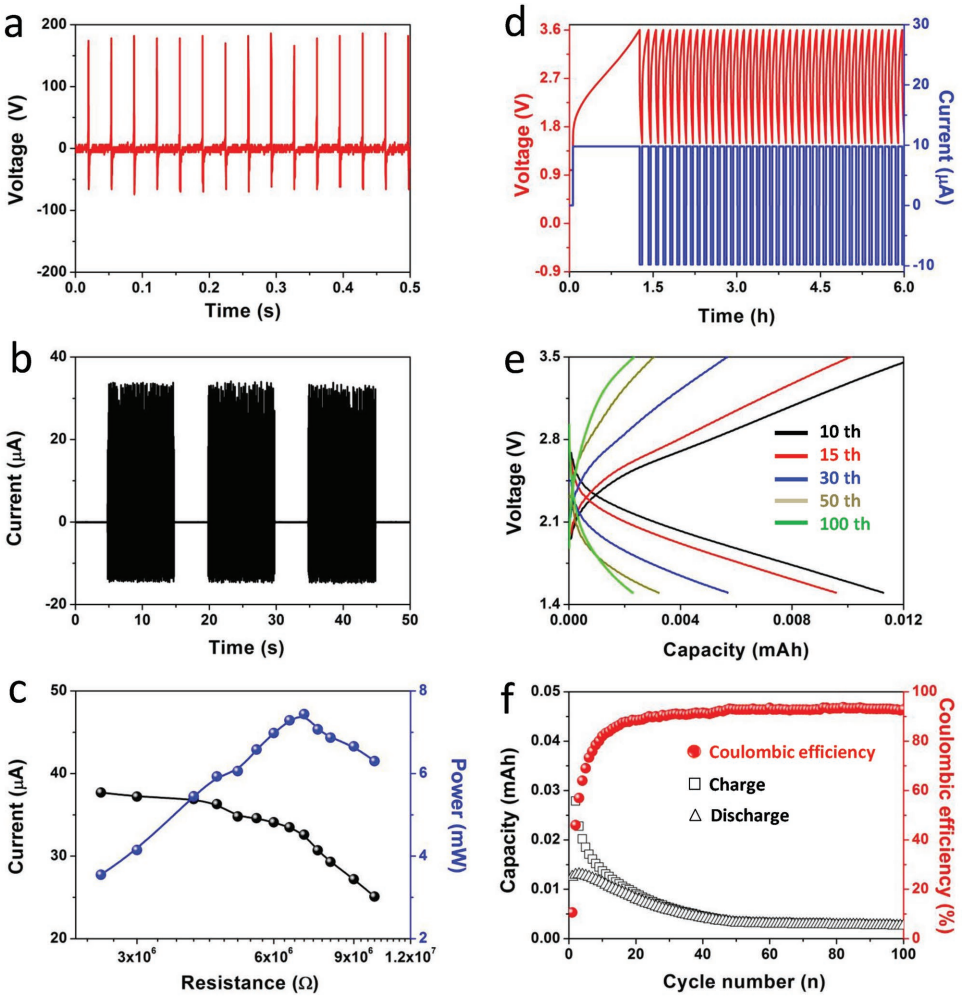

Figure 3. Electrical performances of the CP device. Measured a) output voltage and b) output current signals of the CP device as a triboelectric nanogenerator. c) Measured output current signals of the CP device as a triboelectric nanogenerator under the different loading resistances and the corresponding output powers. d) Measured charging–discharging curves of the CP device as a solid Li-ion battery with a voltage limit between 1.5 and 3.6 V at a current of 0.01 mA. e) Measured galvanostatic charging–discharging curves of the CP device as a solid Li-ion battery under the different cycles. f) Cycling performances and coulombic efficiencies of the CP device as a solid Li-ion battery.

nanotubes and the PEO–LATP electrolyte film can be realized by applying a constant pressure.

The Li-ion charging process of the CP device as an SLB is accomplished by using a TENG charged capacitor, as demonstrated in Figure 2e. The Li ions can migrate from the bottom $LiMn_2O_4$ to the top TiO_2 nanotubes through the solid PEO–LATP electrolyte. The decreased concentration of Li ions at the $LiMn_2O_4$ cathode can result in the chemical reaction ($LiMn_2O_4 \rightarrow Li_{1-x}Mn_2O_4 + xLi^+ + xe^-$), leaving the $Li_{1-x}Mn_2O_4$ at the cathode. The chemical reaction at the TiO_2 anode ($TiO_2 + xLi^+ + xe^- \rightarrow Li_xTiO_2$) enables Li ions to react with TiO_2. In this process, the Li ions can continuously migrate from the $LiMn_2O_4$ cathode to the TiO_2 anode until the voltage of the power source is equal to the charged voltage of the SLB. Figure 2f depicts the discharging process of the CP device as an SLB when a loading resistance was connected to the SLB. The chemical reactions at the TiO_2 anode ($Li_xTiO_2 \rightarrow TiO_2 + xLi^+ + xe^-$) and at the $LiMn_2O_4$ cathode ($Li_{1-x}Mn_2O_4 + xLi^+ + xe^- \rightarrow LiMn_2O_4$) can result in the movement of electrons from the top Ti electrode to the bottom Al electrode. Moreover, the Li ions can migrate from the TiO_2 anode to the $LiMn_2O_4$ cathode, which is the discharging process of the SLB. The triboelectric charges cannot affect the migration of Li-ions in the PEO–LATP electrolyte film under the charging and discharging processes since the triboelectric charges with opposite polarities are fully balanced, as displayed in Figure 2e,f.

Under applied periodical pressures on the device, the CP device can work as a TENG for scavenging ambient mechanical energy. When there is no PEP film in the CP device, we found that the output voltage of the device is smaller than 2 V under a vibration frequency of about 28.3 Hz due to the similar triboelectric polarities of TiO_2 nanotubes and the PEO–LATP electrolyte (Figure S5, Supporting Information), which is difficult to realize the effective charging of Li-ion batteries. To increase the output performance of the TENG and ensure the working of the SLB, an annular FEP film was attached on the PEO–LATP electrolyte. As a result, the output voltage of the TENG can be up to 188 V (**Figure 3**a), giving over 93-fold enhancement.

As displayed in Figure 3b, the output current of the TENG without a loading resistance can be up to 33.5 μA, which clearly decreases with increasing the loading resistances, as depicted in Figure 3c. The corresponding largest output power of the TENG can be up to 7.4 mW under a loading resistance of about 7 MΩ.

The CP device is not only a TENG but also an SLB, where the two different functional devices have the same electrodes. Under applied constant pressures, the TiO_2 nanotubes in the top layer and the PEO–LATP electrolyte in the bottom layer can be in contact with each other, so that the CP device is an SLB. Figure 3d displays the charging–discharging voltage and current curves of the CP device with the voltages ranging from 1.5 to 3.6 V after the first cycle under a charging current of 0.01 mA and a constant pressure of about 20 kg cm^{-2}. Figure 3e presents the charging–discharging curves of the CP device, clearly showing both the charging and discharging capacities decreases with increasing cycles. The charging–discharging capacities and the corresponding coulombic efficiencies under the different cycles are illustrated in Figure 3f. The increase of the charging–discharging times results in an obvious decrease of the capacity in the first 20 cycles and the charging–discharging performance of the CP device becomes to be stable after 40 cycles, where the stable charging capacity is about 3.9 μA h. However, the obtained coulombic efficiency increases with increasing cycles, where it is larger than 90% after 100 cycles.

Although the invented CP device is not only an SLB but also a TENG, we found that the SLB cannot be directly charged by the TENG due to the high AC output voltages of the TENG. To realize that the CP device can generate and store the electric energy by itself, a designed external circuit including a transformer, a rectifier, a capacitor, and six switches has been used, as illustrated in Figure S6 in the Supporting Information. When the periodical pressures were applied on the CP device, the TENG is working. by turning on the switches S1–S4, the high voltages of the TENG can be decreased to smaller than 20 V (Figure S7a, Supporting Information) by using the transformer, resulting in the enhancement of the corresponding output current. The rectifier has been used to convert the AC signals into DC output (Figure S7b, Supporting Information), where the corresponding current outputs are larger than 0.25 mA. Moreover, the decrease of impedance can be confirmed by measuring the output current signals under the different loading resistances (Figure S8, Supporting Information). The designed circuit consists of a transformer, a rectifier, a capacitor, and four switches, as displayed in **Figure 4**a. The harvested energy by using the CP device as a TENG can be effectively stored in the capacitor after using the transformer and the rectifier, where the transformer was utilized to increase output current of TENG and the rectifier was used to convert AC to DC signals. As illustrated in Figure 4b, the different capacitors can be effectively charged by the CP device when the TENG is working under a vibration frequency of about 28.3 Hz. The capacitor with larger capacity requires more charging time, where a 6600 μF capacitor can be charged from 0 to 3 V in about 150 min.

When a constant pressure was applied on the CP device, there is no output for the TENG. The stored electric energy in the capacitor can be utilized to charge the SLB when the switches S5 and S6 were turned on and the switches S1–S4 were turned off, as presented in Figure 4c. Figure 4d displays the charging–discharging curves of the CP device by using the TENG charged capacitor to charge the SLB. When the charging switches are turned on, the charging voltage increases rapidly to 3 V and then decreases with increasing the connecting time. The decrease of the voltage is due to the transfer of electric energy from the charged capacitor to the SLB. Under the same charging time of about 5 min, we found that the capacitor with larger capacity can charge the SLB to a higher voltage. For example, a 940 μF capacitor with a charged voltage of about 3 V can charge the Li-ion battery to about 1.3 V in 5 min, while a 6600 μF capacitor with a charged voltage of about 3 V can charge the Li-ion battery up to 2 V. To confirm the charged electric energy in the CP device, we performed the discharging measurements with a constant discharging current of 0.01 mA. Without the connection between the 6600 μF capacitor and the CP device after being charged in 5 min, the voltage of the CP device can sustain in about 240 s from 2 to 0.9 V under the discharging current of 0.01 mA, indicating that the electric energy can be effectively stored in the CP device. As a result, the CP device can generate and store electric energy by itself.

We first demonstrated that the CP device can be utilized to directly light up a green LED. As presented in **Figure 5**a, a green LED can be lighted up by the CP device when a human hand was used to apply periodical pressures on it to drive the working of the TENG, as displayed in Movie S1 in the Supporting Information. Moreover, when the CP device under a constant pressure of about 20 kg cm^{-2} after being charged can also be utilized to continuously light up a green LED, as illustrated in Figure 5b and Movie S2 (Supporting Information). To understand the relationship between the capacity of the Li-ion battery and the applied pressure, the charging–discharging performances of the SLB after 100 cycles under the different pressures were measured (Figure S9, Supporting Information). As displayed in Figure 5c, both the charging and discharging capacities of the SLB increase with increasing the loading pressures ranged from 0 to 30 kg cm^{-2}, where the corresponding charging and discharging capacities are about 14.3 and 13.2 μA h, respectively. The reason for the increase of capacities is associated with the pressure induced close contact between the TiO_2 nanotubes and PEO–LATP electrolyte, which can be beneficial for Li-ion migrations.

To verify whether the Li-ion battery can be applied in wearable electronics, we measured the charging–discharging performances of the Li-ion battery under the pressure of a human body with a weight of about 55 kg, as depicted in Figure 5d. Under the charging–discharging current of 5 μA, the first charging and discharging capacities are 1.9 and 0.2 μAh, respectively. After this, the charging and discharging capacities can be stable at 0.7 and 0.3 μAh, respectively. These results indicate that the SLB can effectively work under the human body induced pressures. After the CP device was mounted in a human shoe (Figure S10a, Supporting Information), we measured the output voltage signals of the TENG when a person was walking, as shown in Figure 5e. When compared with slow walking, fast walking leads to more voltage peaks, which can generate more electric energy. Moreover, the corresponding output current of the TENG under the fast walking

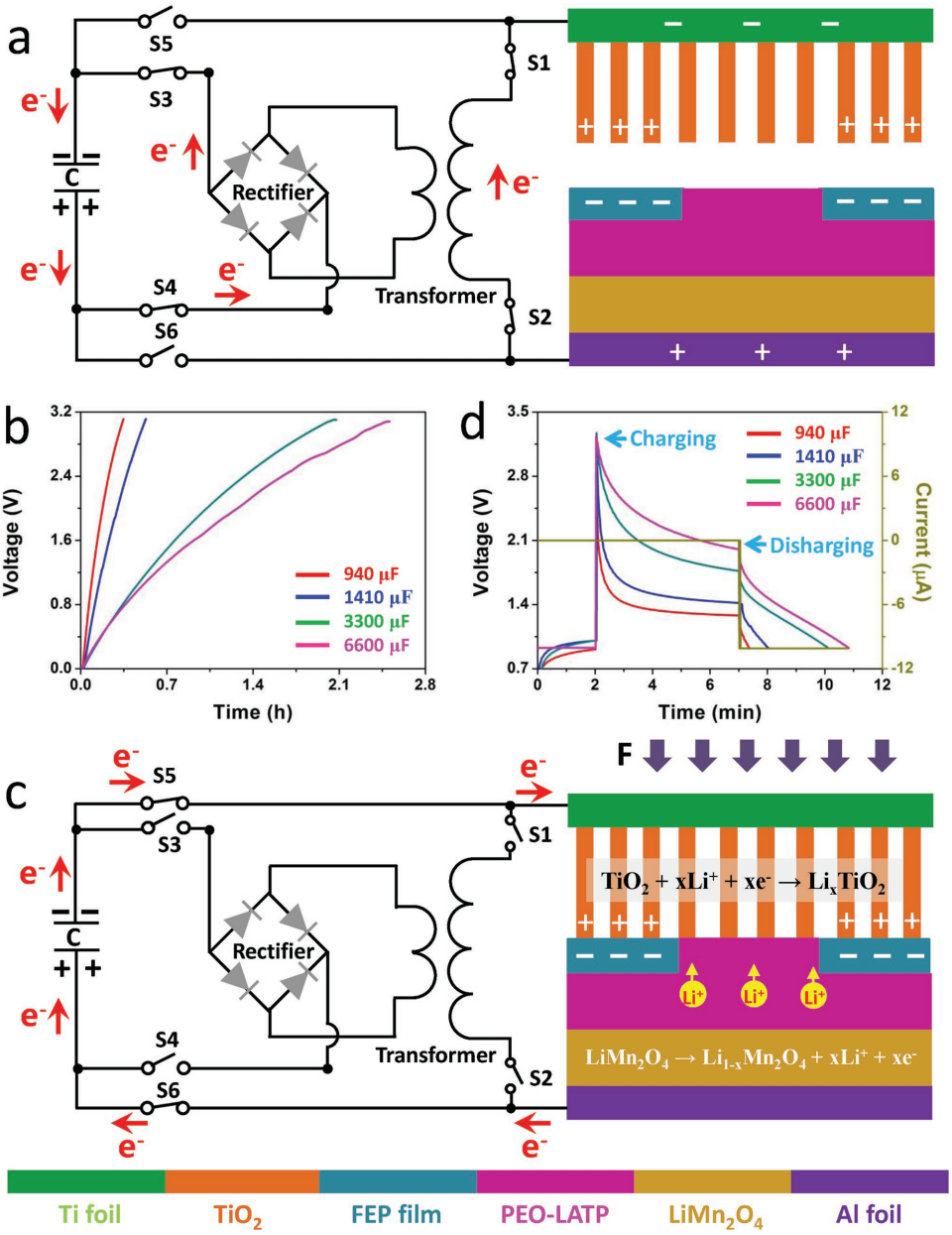

Figure 4. Self-charging process of the CP device by using a designed circuit. a) Schematic illustration of the designed circuit and electricity transfer from the CPD device to the capacitor in the external circuit. b) Charging curves of the different capacitors by using the CP device as a TENG by using the designed circuit in (a). c) Schematic illustration of the electric storage process from the external capacitor to the CPD device as an SLB. d) Charging–discharging curves of the CP device as an SLB by using the different capacitors charged by the CP device as a TENG.

is larger than that under the slow walking (Figure S10b,c, Supporting Information). As a result, the CP device in the human shoe under the fast walking can charge an Li-ion battery to a higher voltage of about 1.12 V in about 5 min as compared with that (1.05 V) under the slow walking, as displayed in Figure 5f. A photograph of a green LED lit up by the CP device as the charged SLB can be clearly observed (Figure S10d and Movie S3, Supporting Information), demonstrating the potential of this device in self-powered wearable electronics.

In summary, we have presented a CP device that effectively conjoins an SLB and a TENG by the internal hybrid, where the two different functional devices share some electrodes. The working of the TENG is based on the coupling between triboelectric effect and electrostatic induction under the periodical contact/separation between TiO_2 nanotubes and the FEP film. The use of the FEP film in CP device can give a 93-fold enhancement in output voltage of the TENG as compared with no use of the FEP film. The TiO_2 nanotubes and the LMO film were utilized as anode and cathode of the SLB, respectively. Under periodical pressures, the CP device is a TENG that can deliver an output voltage of about 188 V and an output current of about 33.5 μA by scavenging the vibration energy. Under the constant

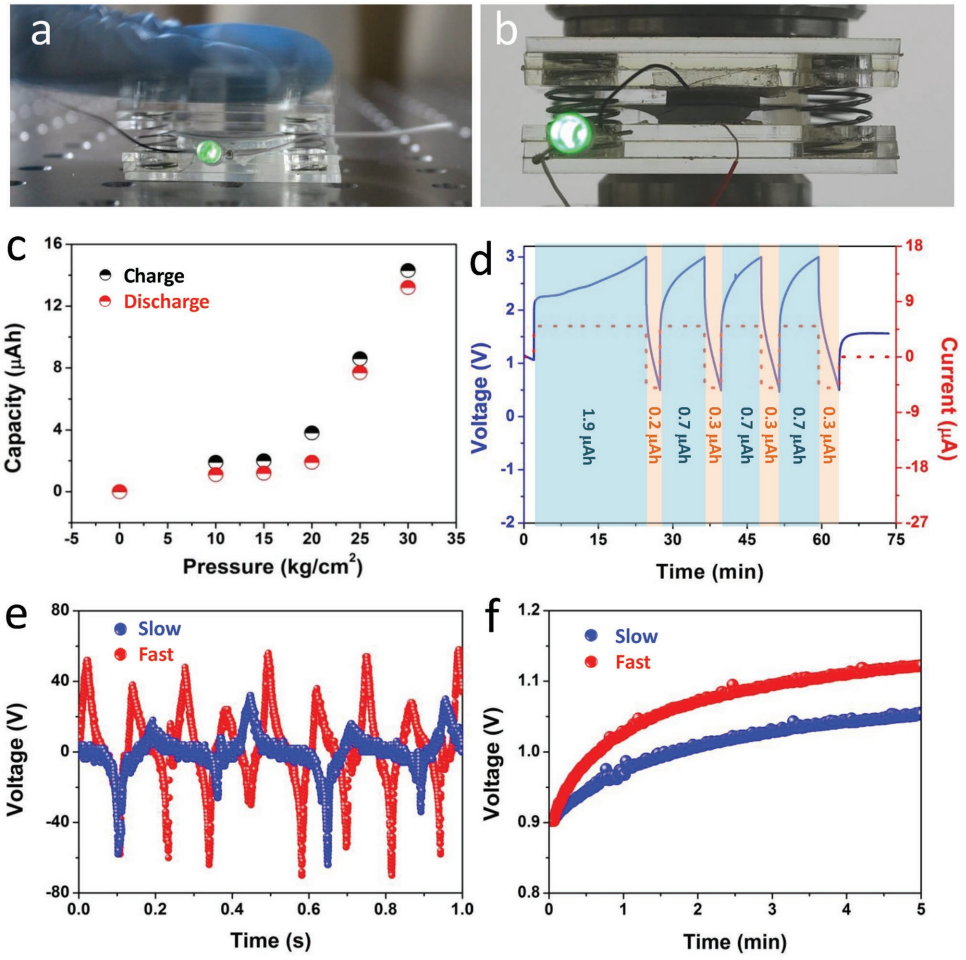

Figure 5. Applications of the CP device in self-powered wearable electronics. Photographs of a green LED that can be lighted up by the CP device as a) a TENG or b) an SLB. c) Charging–discharging capacities of the CP device as an SLB after 100 cycles under the different loading pressures. d) Charging–discharging curves of the CP device as a solid Li-ion battery under the pressure induced by a human body with a weight of about 55 kg. e) Measured output voltage signals of the CP device as a TENG driven by human walking. f) Charging curves of another CP device as an SLB by using the produced electric energy in (e).

pressures, the CP device is an SLB that can be utilized to store electric energy, where the corresponding charging–discharging capacities can be increased by increasing the applied pressures. Both the TENG and the SLB can be utilized to directly light up a green LED. The invented CP device can be integrated into a human shoe for scavenging and storing energy from human walking, demonstrating the potential applications in self-powered wearable electronics.

Experimental Section

Preparation of TiO_2 Nanotubes and $LiMn_2O_4$ Electrodes: The TiO_2 nanotubes were prepared by electrochemically anodizing Ti foil with the thickness of about 0.05 mm in ethylene glycol solution that included 1.5 g NH_4F and 10 g H_2O with another Ti foil as a counter electrode. Before anodization, both sides of the Ti foil were ultrasonically cleaned in 13% hydrochloric acid solution, acetone, and ethanol for 10 min, respectively, and then dried in air. The prepared Ti foil was first anodized at 60 V for 0.5 h. The obtained nanotube films on both sides of the foil were then removed by ultrasonication in distilled water for a few minutes. A second anodization was then performed at 50 V for 1 h to produce TiO_2 nanotubes on the top. The $LiMn_2O_4$ electrode was prepared in aqueous solution, where $LiMn_2O_4$, polyvinylpyrrolidone, and acetylene black were first mixed at a mass ratio of 8:1:1 in distilled water to form a slurry. The slurry was then pasted on an Al foil and dried at 80 °C. After that, it was dried in vacuum at 100 °C for 24 h.

Preparation of $Li_{(1+x)}Ti_{(2-x)}Al_x(PO_4)_3$: The synthesis process of $Li_{(1+x)}Ti_{(2-x)}Al_x(PO_4)_3$ was based on the following processes. A stoichiometric amount of $Ti(OC_4H_9)_4$ was first dissolved into the mixture of deionized water and concentrated nitric acid with the volume ratio of 4:1, where the mixed solution was continuously stirred with a magnetic stirrer to obtain a homogenous solution. The purpose for the use of HNO_3 was to inhibit the hydrolysis of $Ti(OC_4H_9)_4$. Subsequently, stoichiometric amounts of $LiNO_3$ and $Al(NO_3)_3{\cdot}9H_2O$ were added into the solution under the condition of continuous stirring until they were completely dissolved. The citric acid monohydrate ($C_6H_8O_7{\cdot}H_2O$) as a complexant was then added to create a transparent solution, where the corresponding molar ratio between $C_6H_8O_7{\cdot}H_2O$ and all metal cations was 1.5:1. The pH value of the obtained solution was adjusted to 5 by utilizing the ammonia solution, and then $NH_4H_2(PO_4)_3$ and ethylene glycol ($C_2H_6O_2$) were dissolved into the solution. The final solution was heated at 180 °C in a blast drying oven to evaporate the excessive water and promote esterification until a black resin was formed.

The resulting solid film was then ground and calcined at 850 °C for 5 h at a heating rate of 2 °C min^{-1} to produce the crystalline LATP powders. The uniform composite PEO–LATP electrolyte membrane with thickness of 210 nm was obtained by a solution-casting method. LATP powders, bistrifluoromethanesulfonimide ($LiN(CF_3SO_2)_2$), and PEO were dissolved in acetonitrile at a mass ratio of 8:1:2. Through continuous stirring, a transparent solution was obtained. Then the resulting solution was poured into a plastic mold, where water was evaporated under ambient conditions. After being dry, the membrane was peeled from the plastic substrate to obtain the PEO–LATP electrolyte membrane.

Fabrication of the CP Device: The whole device had a dimension of 60 mm × 60 mm × 30 mm, where two layers were separated by four springs at the corners. Two acrylic plates with a diameter of 30 mm and a height of 2 mm were attached on the bottom substrate. The PEO–LATP–LMO membrane which was made under the pressure of 15–20 MPa and the TiO_2 nanotube foil were cut into a cycle with a diameter of 30 mm and then attached on the top acrylic plate. An FEP circular membrane of 30 mm diameter and 15 mm inner diameter was utilized as one triboelectric material, which was fixed on the surface of the PEO–LATP–LMO membrane.

Characterizations and Measurements: The charging–discharging performances of the SLBs were characterized by using an MTI 8 channels battery analyzer (CTS8-5 V 1 mA). The morphologies of the TiO_2 nanotubes and the LATP nanoparticles were characterized using a field-emission scanning electron microscope (SU8020). The crystal structure of the LATP film was identified by XRD by using Cu Kα radiation. The output voltage and current signals of the TENGs were measured by a mixed domain oscilloscope (Tektronix MDO3024) and a low-noise current preamplifier (Stanford Research SR570), respectively.

Supporting Information

Supporting Information is available from the Wiley Online Library or from the author.

Acknowledgements

This work was supported by the National Natural Science Foundation of China (Grant Nos. 51472055 and 61404034), External Cooperation Program of BIC, Chinese Academy of Sciences (Grant No. 121411KYS820150028), the 2015 Annual Beijing Talents Fund (Grant No. 2015000021223ZK32), the National Key R&D Program of China (Grant No. 2016YFA0202701), and the "thousands talents" program for the pioneer researcher and his innovation team, China. The corresponding patent based on this work has been submitted.

Conflict of Interest

The authors declare no conflict of interest.

Keywords

hybrid structures, self-powered electronics, solid Li-ion batteries, triboelectric nanogenerators, wearable electronics

Received: June 14, 2017
Revised: July 4, 2017
Published online:

[1] K. I. Jang, S. Y. Han, S. Xu, K. E. Mathewson, Y. Zhang, J. W. Jeong, G. T. Kim, R. C. Webb, J. W. Lee, T. J. Dawidczyk, R. H. Kim, Y. M. Song, W. H. Yeo, S. Kim, H. Cheng, S. Rhee, J. Chung, B. Kim, H. U. Chung, D. Lee, Y. Yang, M. Cho, J. G. Gaspar, R. Carbonari, M. Fabiani, G. Gratton, Y. Huan, J. A. Rogers, *Nat. Commun.* **2014**, *5*, 4779.
[2] C. Degdeviren, Y. Su, P. Joe, R. Yona, Y. Liu, Y. S. Kim, Y. Huang, A. R. Damadoran, J. Xia, L. W. Martin, Y. Huan, J. A. Rogers, *Nat. Commun.* **2014**, *5*, 4496.
[3] Z. L. Wang, J. Song, *Science* **2006**, *312*, 242.
[4] Y. Yang, W. Guo, K. C. Pradel, G. Zhu, Y. Zhou, Y. Zhang, Y. Hu, L. Lin, Z. L. Wang, *Nano Lett.* **2012**, *12*, 2833.
[5] J. M. Donelan, Q. Li, V. Naing, J. A. Hoffer, D. J. Weber, A. D. Kuo, *Science* **2008**, *319*, 807.
[6] J. Chun, B. U. Ye, J. W. Lee, D. Choi, C. Y. Kang, S. W. Kim, Z. L. Wang, J. M. Baik, *Nat. Commun.* **2016**, *7*, 12985.
[7] K. Zhang, Z. L. Wang, Y. Yang, *ACS Nano* **2016**, *10*, 4728.
[8] F. R. Fan, Z. Q. Tian, Z. L. Wang, *Nano Energy* **2012**, *1*, 328.
[9] H. Guo, J. Chen, L. Tian, Q. Leng, Y. Xi, C. Hu, *ACS Appl. Mater. Interfaces* **2014**, *6*, 17184.
[10] S. Wang, X. Mu, Y. Yang, C. Sun, A. Y. Gu, Z. L. Wang, *Adv. Mater.* **2015**, *27*, 240.
[11] Y. Yang, Y. S. Zhou, H. Zhang, Y. Liu, S. Lee, Z. L. Wang, *Adv. Mater.* **2013**, *25*, 6594.
[12] X. Wang, S. Wang, Y. Yang, Z. L. Wang, *ACS Nano* **2015**, *9*, 4553.
[13] J. Chuang, S. Lee, H. Yong, H. Moon, D. Choi, S. Lee, *Nano Energy* **2016**, *20*, 84.
[14] T. Quan, X. Wang, Z. L. Wang, Y. Yang, *ACS Nano* **2015**, *9*, 12301.
[15] X. Xia, G. Liu, H. Guo, Q. Leng, C. Hu, Y. Xi, *Nano Energy* **2015**, *15*, 766.
[16] X. Pu, M. Liu, L. Li, C. Zhang, Y. Pang, C. Jiang, L. Shao, W. Hu, Z. L. Wang, *Adv. Sci.* **2016**, *3*, 1500255.
[17] T. Quan, Y. Yang, *Nano Res.* **2016**, *9*, 2226.
[18] X. Pu, L. Li, H. Song, C. Du, Z. Zhao, C. Jiang, G. Cao, W. Hu, Z. L. Wang, *Adv. Mater.* **2015**, *27*, 2472.
[19] H. Wu, G. Yu, L. Pan, N. Liu, M. T. Mcdowell, Z. Bao, Y. Cui, *Nat. Commun.* **2013**, *4*, 1943.
[20] L. Hu, N. Liu, M. Eskilsson, G. Zheng, J. McDonough, L. Wagberg, Y. Cui, *Nano Energy* **2013**, *2*, 138.
[21] Y. Liu, D. Lin, P. Y. Yuen, K. Liu, J. Xie, R. H. Dauskardt, Y. Cui, *Adv. Mater.* **2017**, *29*, 1605531.
[22] D. Lin, W. Liu, Y. Liu, H. R. Lee, P. C. Hsu, K. Liu, Y. Cui, *Nano Lett.* **2016**, *16*, 459.